# Propagation Graph Modeling of Time-Varying Radio Channels

Stern, Kristoffer; Fuglsig, Andreas Jonas; Ramsgaard-Jensen, Kasper; Pedersen, Troels

# Propagation Graph Modeling of Time-Varying Radio Channels

Kristoffer Stern*, Andreas Jonas Fuglsig*, Kasper Ramsgaard-Jensen* and Troels Pedersen**
*Study board of mathematics, physics and nano-technology, Aalborg University, DK-9220 Aalborg East, Denmark
*Email: {kstern14, afugls14, kramsg14}@student.aau.dk
** Department of Electronic Systems, Aalborg University, DK-9220 Aalborg East, Denmark
**Email: troels@es.aau.dk

*Abstract*—Radio systems operating in time-varying propagation environments are exposed to rapid fading in the transfer function due to multi-path effects. In general propagation environments, where recursive scattering may occur, modeling and simulating the channel is challenging. In this contribution, we model the channel as a time-varying propagation graph induced by vertices representing transmitters, receivers and scatterers and edges representing the propagation conditions between the vertices. For time-varying systems a closed form expression for the transfer matrix of the graph is not available and therefore we introduce an approximation by assuming the graph model to be an approximately underspread system. We give a bound for the resulting approximation error. Finally, simulations illustrate how the model can be applied for simulation of a vehicle-to-vehicle tunnel scenario with time-varying delays and Doppler-shifts.

## I. INTRODUCTION

A widespread modeling technique of time-dynamic radio channels such as vehicular radio channels is the geometry-based stochastic channel models (GSCMs) [1] where the propagation environment is represented via a number of propagation paths. These paths are defined by scatterers placed geometrically according to a particular propagation environment or defined in a stochastic manner. However, it is difficult to account for reverberation effects which occur in many propagation scenarios, e.g. in tunnels or street canyons.

As an alternative, [2]–[4] the environment can be modeled by means of a so-called propagation graph in which transmitters, receivers and scatterers are represented by vertices and the propagation conditions as edges. As in a GSCM, vertices of a propagation graph may be placed according to geometry. In contrast to the GSCM, a propagation graph allows for modeling of recursive scattering, thus accounting for reverberation effects giving rise to a diffuse multipath component. Propagation graphs have previously been considered for modeling the time-invariant case with static vertices [4]. Each edge is weighted by a transfer function describing the delay and gain of the signal propagating along the specific edge. For the time-invariant case, the resulting transfer function for the entire propagation graph is presented with a closed form solution. In [5] and [6] this model has been used to describe a time-varying radio channel considering a high-speed train scenario. In both of these contributions, the adaptation to time-variation is done by only regarding one or two interactions of the signal before reaching the receiver. In [7] a hybrid model combining ray tracing and propagation graphs is proposed for vehicle-to-vehicle communication in a

tunnel. The mathematical soundness of this approach, however, is still not investigated.

In this contribution, we generalize the propagation graph model [4] into the framework of time-varying graphs [8]. This generalization involves the possibility for edges appearing and disappearing as time progresses. Furthermore, the signal transfer along each edge should be described as a Linear Time-Variant (LTV) system. Unfortunately the multiplicative property of transfer functions known from the time-invariant case is in general not valid for time-varying systems.

Therefore we explore conditions for which the transfer function can be achieved via multiplicative calculus and give a bound for the approximation errors introduced in the model. Finally, we give two simulation examples considering a vehicle-to-vehicle (V2V) channel in a particular tunnel scenario.

## II. TIME-VARYING PROPAGATION GRAPHS

We represent the propagation environment as a time-varying graph, allowing recursive and nonrecursive scattering as well as changing propagation conditions. We follow [8] in which the notion of a time-varying graph is defined along with related concepts. Consider a directed graph, $G = (V, E)$, without multiple edges between vertices. Now we let the set of edges, $E$, be time-varying in the sense that the time it takes to traverse an edge can vary, and the edges can come and go. Formally we define a time-varying graph, $\mathcal{G} = (V, E, \mathcal{T}, \rho, \tau)$, as a finite nonempty set of vertices, $V$, with a set of edges, $E \subseteq V^2$. The graph $\mathcal{G}$ is defined over a time span, $\mathcal{T} \subseteq \mathbb{T}$, called the *lifetime* of the graph, where $\mathbb{T}$ is an arbitrary temporal domain. The *edge presence function*, $\rho : E \times \mathcal{T} \to \{0, 1\}$, indicates whether a given edge is present at a given time, $t$. The time it takes to traverse an edge is given by the *edge delay function*, $\tau : E \times \mathcal{T} \to \mathbb{T}$. The directed graph containing all edges that appear throughout the lifetime of $\mathcal{G}$ is called the *underlying graph* of $\mathcal{G}$. For a time-varying graph $\mathcal{G}$ of order $N$, the *time-varying adjacency matrix* $\mathbf{A}(t) \in \mathbb{R}^{N \times N}$, is the zero-one matrix

$$[\mathbf{A}(t)]_{i,j} = \begin{cases} \rho((v_j, v_i), t), & \text{if } (v_j, v_i) \in E \\ 0, & \text{otherwise.} \end{cases} \quad (1)$$

The concept of a path in a static graph can be generalized to the dynamic case by defining a *(direct) journey* [8]. A direct journey, $\mathcal{J}$, in $\mathcal{G}$ is a finite sequence $\{(e_1, t_1), (e_2, t_2), \ldots, (e_k, t_k)\}$ with three properties
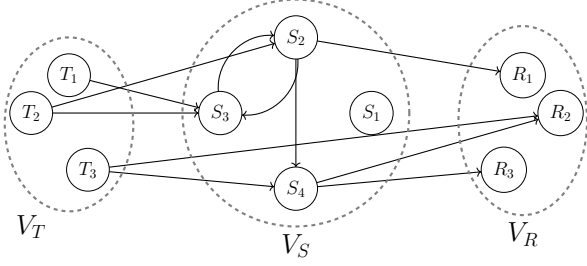
Fig. 1. Example of a time-varying propagation graph at time $t = t'$.

(i) $\{e_1, e_2, \ldots, e_k\}$ is a walk in the underlying graph of $\mathcal{G}$

(ii) $\rho(e_i, t) = 1 \ \forall \ t \in [t_i, t_i + \tau(e_i, t_i)]$, for $1 \leq i < k$

(iii) $\tau(e_i, t_i)$ is such that $t_{i+1} = t_i + \tau(e_i, t_i)$ for $1 \leq i < k$.

Property (iii) ensures the next edge in the journey can be crossed immediately, i.e. there is no waiting involved.

A time-varying propagation graph can now be defined. Following [4], we let the vertices of the graph represent transmitters, receivers and scatterers, see Figure 1. The propagation conditions are represented by the present edges. Thus if there is an edge between a transmitter and a receiver direct propagation occurs. The sets $V_T = \{T_1, \ldots, T_n\}$, $V_S = \{S_1, \ldots, S_k\}$ and $V_R = \{R_1, \ldots, R_m\}$ are the sets of transmitters, scatterers and receivers. Furthermore $E_D = E \cap (V_T \times V_R)$, $E_T = E \cap (V_T \times V_S)$, $E_S = E \cap (V_S \times V_S)$ and $E_R = E \cap (V_S \times V_R)$ are the sets of edges between: Transmitters and receivers, transmitters and scatterers, scatterers in-between, and scatterers and receivers. A time-varying propagation graph is defined as the time-varying graph $\mathcal{G} = (V, E, \mathcal{T}, \rho, \tau)$ with $V = V_T \cup V_S \cup V_R$ and $E = E_D \cup E_T \cup E_S \cup E_R$. For all pairs $v, v' \in V$ and $e = (v, v')$ the edge presence function $\rho(e, t) = 1$ if a signal can propagate from $v$ to $v'$ at time $t$, and the edge delay function, $\tau(e, t)$, describes the propagation time from $v$ to $v'$ at time $t$. We define a *propagation journey* as a direct journey in a time-varying propagation graph.

Each edge in the time-varying propagation graph represents an LTV *Hilbert-Schmidt* operator, $\mathcal{O} : L_2(\mathbb{R}) \to L_2(\mathbb{R})$, cf [9]–[11]. We assign each edge, $e$, in the underlying graph a time-varying transfer function $H_e(t, f)$. Thus the time-varying propagation graph can be described by a weighted time-varying adjacency matrix $\mathbf{A}(t, f) \in \mathbb{C}^{(N_T + N_R + N_S) \times (N_T + N_R + N_S)}$ with entries

$$[\mathbf{A}(t, f)]_{ij} = \begin{cases} H_{(v_j, v_i)}(t, f), & \text{if } \rho((v_j, v_i), t) = 1 \\ 0, & \text{otherwise.} \end{cases} \quad (2)$$

As no edges enter transmitters or leave receivers the first $N_T$ rows and $N_T + 1, \ldots, N_T + N_R$ columns of $\mathbf{A}(t, f)$ are zero. By properly indexing the vertices,

$$\mathbf{A}(t, f) = \begin{bmatrix} \mathbf{0} & \mathbf{0} & \mathbf{0} \\ \mathbf{D}(t, f) & \mathbf{0} & \mathbf{R}(t, f) \\ \mathbf{T}(t, f) & \mathbf{0} & \mathbf{B}(t, f) \end{bmatrix}, \quad (3)$$

where $\mathbf{D}(t, f)$, $\mathbf{R}(t, f)$, $\mathbf{T}(t, f)$ and $\mathbf{B}(t, f)$ are the time-varying transfer matrices describing propagations between

transmitter-receiver, scatterer-receiver, transmitter-receiver and scatterer-scatterer respectively. That is

$$\mathbf{D}(t, f) \in \mathbb{C}^{N_R \times N_T} \quad \text{connecting } V_T \text{ to } V_R, \quad (4a)$$
$$\mathbf{R}(t, f) \in \mathbb{C}^{N_R \times N_S} \quad \text{connecting } V_S \text{ to } V_R, \quad (4b)$$
$$\mathbf{T}(t, f) \in \mathbb{C}^{N_S \times N_T} \quad \text{connecting } V_T \text{ to } V_S, \quad (4c)$$
$$\mathbf{B}(t, f) \in \mathbb{C}^{N_S \times N_S} \quad \text{interconnecting } V_S. \quad (4d)$$

Denote the input signal vector in the Fourier domain as $\mathbf{X}(f)$ and the received signal by $\mathbf{y}(t)$. The input output relation of a propagation graph then reads

$$\mathbf{y}(t) = \int_{-\infty}^{\infty} \mathbf{H}(t, f) \mathbf{X}(f) e^{i2\pi ft} \mathrm{d}f \quad (5)$$

where $\mathbf{H}(t, f)$ is the $N_R \times N_T$ time-varying transfer matrix of the propagation graph [9]. The transfer matrix $\mathbf{H}(t, f)$ is given as

$$\mathbf{H}(t, f) = \sum_{k=0}^{\infty} \mathbf{H}_k(t, f), \quad (6)$$

where $\mathbf{H}_k$ is the transfer matrix of propagation journeys of length $k$. Then entry $(v', v)$ of $\mathbf{H}_k(t, f)$ is the superposition of the transfer function of each journey from $v$ to $v'$. Denote by $\mathcal{J}_{vv'}^k$ the set of all possible propagation journeys of length $k$ from $v$ to $v'$, then

$$[\mathbf{H}_k(t, f)]_{(v', v)} = \sum_{j \in \mathcal{J}_{vv'}^k} H_j(t, f), \quad (7)$$

where $H_j(t, f)$ is the transfer function of the cascade of LTV operators in journey $j$.

### III. UNDERSPREAD LTV SYSTEMS

To compute the transfer function in (7) a convenient method for obtaining the transfer function of sums and cascades of LTV operators is needed. To this end, we consider a special type of operators, called *underspread* operators, which are approximately time- and frequency-invariant. For an underspread operator $\mathcal{O}_j$, with kernel $h_j$, the *delay-Doppler-spread function*,

$$S_{\mathcal{O}_j}(\tau, \nu) := \int_{-\infty}^{\infty} h_j(t, t - \tau) e^{-i2\pi\nu t} \mathrm{d}t, \quad (8)$$

has support contained in $[-\tau_j, \tau_j] \times [-\nu_j, \nu_j]$ and

$$4\tau_j \nu_j \ll 1, \quad (9)$$

where $\tau_j$ and $\nu_j$ are the maximal absolute time and frequency shifts of the operator $\mathcal{O}_j$ [9]. Similarly operators $\mathcal{O}_1, \ldots, \mathcal{O}_N$ are said to be *jointly underspread* if $4\tau_{\max}\nu_{\max} \ll 1$, where $\tau_{\max} = \max\{\tau_1, \ldots, \tau_N\}$ and $\nu_{\max} = \max\{\nu_1, \ldots, \nu_N\}$.

The delay-Doppler-spread function of a sum of operators is by linearity the sum of the individual delay-Doppler-spread functions. Since the jointly underspread operators are zero outside $[-\tau_{\max}, \tau_{\max}] \times [-\nu_{\max}, \nu_{\max}]$ the sum of delay-Doppler-spread functions of jointly underspread operators is also zero outside this interval preserving the underspread property. This is the case for the sum of infinitely many jointly underspread operators.

A cascade of underspread operators does not preserve the underspread property in the same way as a sum. Consider a

cascade of operators, $\mathcal{C}_2 : \mathcal{O}_1\mathcal{O}_2$. The delay-Doppler-spread function of $\mathcal{C}_2$ is given as [9]

$$S_{\mathcal{C}_2}(\tau,\nu):= \int_{-\infty}^{\infty} \int_{-\infty}^{\infty} S_{\mathcal{O}_1}(\tau',\nu') S_{\mathcal{O}_2}(\tau-\tau',\nu-\nu') \\ \cdot e^{-i2\pi(\tau'\nu-\tau'\nu')} d\tau' d\nu'. \quad (10)$$

The delay-Doppler-spread function of any order cascade, $\mathcal{C}_N : \mathcal{O}_1 \cdots \mathcal{O}_N$ can be computed by iteration of (10). We seek conditions for when the cascade $\mathcal{C}_N$, is itself underspread. Define

$$\tau^{(N)} = \tau_1 + \tau_2 + \cdots + \tau_N, \quad (11)$$
$$\nu^{(N)} = \nu_1 + \nu_2 + \cdots + \nu_N. \quad (12)$$

From (10) it appears that the support of the delay-Doppler-spread function of two operators in cascade, $S_{\mathcal{C}_2}$, is limited to $[-\tau^{(2)},\tau^{(2)}] \times [-\nu^{(2)},\nu^{(2)}]$. From iteration of (10) it follows that the support of $S_{\mathcal{C}_N}$ is contained in $[-\tau^{(N)},\tau^{(N)}] \times [-\nu^{(N)},\nu^{(N)}]$. Therefore if $\tau^{(N)}$ and $\nu^{(N)}$ fulfills that $4\tau^{(N)}\nu^{(N)} \ll 1$, the cascade $\mathcal{C}_N$ is underspread. When adding more operators to the cascade. i.e. increasing $N$, then $\tau^{(N)}$ and $\nu^{(N)}$ increases, and for $N \to \infty$ the cascade will not be underspread. We are therefore limited to consider finite length cascades.

Kozek [9] showed that for two operators $\mathcal{O}_1$ and $\mathcal{O}_2$ with $2\max(\tau_1,\tau_2)\max(\nu_1,\nu_2) \le 1$, the time-varying transfer function $H_{\mathcal{C}_2}$ of the cascade $\mathcal{C}_2$ can be approximated by the multiplication of the individual transfer functions $H_{\mathcal{O}_1}, H_{\mathcal{O}_2}$,

$$H_{\mathcal{C}_2}(t,f) \approx H_{\mathcal{O}_1}(t,f) H_{\mathcal{O}_2}(t,f), \quad (13)$$

with the approximation error bounded as:

$$|H_{\mathcal{C}_2} - H_{\mathcal{O}_1}H_{\mathcal{O}_2}| < 2\sin(2\pi\tau_0\nu_0)||S_{\mathcal{O}_1}||_1||S_{\mathcal{O}_2}||_1, \quad (14)$$

where $\tau_0 = \max(\tau_1,\tau_2)$ and $\nu_0 = \max(\nu_1,\nu_2)$. The restriction on $\tau_1,\tau_2,\nu_1$ and $\nu_2$ are strictly satisfied for jointly underspread operators, thus making the approximation (13) valid. We now give a sufficient condition for generalizing this to longer cascades.

*Theorem 1:* For a cascade, $\mathcal{C}_N$, of $N \ge 1$ jointly underspread Hilbert-Schmidt operators with $4\tau^{(N)}\nu^{(N)} < 1$ the approximation error $|H_{\mathcal{C}_N} - H_{\mathcal{O}_1}H_{\mathcal{O}_2}\cdots H_{\mathcal{O}_N}|$ of the transfer function is bounded as

$$|H_{\mathcal{C}_N} - H_{\mathcal{O}_1}\cdots H_{\mathcal{O}_N}| \le 2(N-1)\sin(\Psi_N)\prod_{i=1}^{N}||S_{\mathcal{O}_i}||_1 \quad (15)$$

where $\Psi_N = 2\pi\tau^{(N)}\nu^{(N)}$ .

*Proof:* For the case of $N = 1$ both sides of (15) are zero. We proceed with a proof by induction. The basis step of $N = 2$ is the case of (14). Consider the case of $N + 1$ and let

$$E_{N+1} = |H_{\mathcal{C}_{N+1}} - H_{\mathcal{O}_1}\cdots H_{\mathcal{O}_{N+1}}|. \quad (16)$$

By the induction hypothesis we can write

$$E_{N+1} = |H_{\mathcal{C}_{N+1}} - (H_{\mathcal{C}_N} + \epsilon) H_{\mathcal{O}_{N+1}}|, \quad (17)$$

where $|\epsilon| \le 2(N-1)\sin(\Psi_N)\prod_{i=1}^{N}||S_{\mathcal{O}_i}||_1$. Then by the triangle- and integral triangle inequality,

$$E_{N+1} \le |H_{\mathcal{C}_{N+1}} - H_{\mathcal{C}_N}H_{\mathcal{O}_{N+1}}| + |\epsilon| \cdot ||S_{\mathcal{O}_{N+1}}||_1. \quad (18)$$

Finally, because $\max(\tau_{\mathcal{C}_N},\tau_{N+1}) \le \tau^{(N+1)}$ and $\max(\nu_{\mathcal{C}_N},\nu_{N+1}) \le \nu^{(N+1)}$ where $4\tau^{(N+1)}\nu^{(N+1)} < 1$, then by (14)

$$E_{N+1} < \quad 2\sin(\Psi_{N+1}) \cdot ||S_{\mathcal{C}_N}||_1||S_{\mathcal{O}_{N+1}}||_1 + \quad (19)$$
$$2(N-1)\sin(\Psi_N)\prod_{i=1}^{N}||S_{\mathcal{O}_i}||_1||S_{\mathcal{O}_{N+1}}||_1$$
$$< 2N\sin(\Psi_{N+1})\prod_{i=1}^{N+1}||S_{\mathcal{O}_i}||_1 \quad (20)$$

∎

Let $N_U$ be the maximum length of a cascade such that it remains underspread. Then the transfer function of all cascades of length less than $N_U$ can be approximated via multiplication. Furthermore this bound can be compared to the error caused by truncating (6) to cascades of length $N_U$. In order to compare these errors we expand the concept of underspread systems to matrices.

Consider a matrix of transfer functions, $\mathbf{H}(t,f)$, representing Hilbert-Schmidt operators. Such matrices have maximum delay $\tau_{\mathbf{H}}$ and maximum Doppler shift $\nu_{\mathbf{H}}$ where for all entries in the matrix the maximum delay and Doppler shift of the respective operator is bounded by $\tau_{\mathbf{H}}$ and $\nu_{\mathbf{H}}$. Two matrices, $\mathbf{H}_1(t,f), \mathbf{H}_2(t,f)$, are said to be jointly underspread if all entries of both matrices are jointly underspread. Let $\tau_0 = \max(\tau_{\mathbf{H}_1},\tau_{\mathbf{H}_2})$ and $\nu_0 = \max(\nu_{\mathbf{H}_1},\nu_{\mathbf{H}_2})$, we call $\tau_0$ and $\nu_0$ the *covering* delay and Doppler shift of $\mathbf{H}_1(t,f)$ and $\mathbf{H}_2(t,f)$.

For a time-varying propagation graph with transfer matrices defined as in (4), let $\mathbf{R}(t,f)$, $\mathbf{B}(t,f)$ and $\mathbf{T}(t,f)$ be jointly underspread with covering delay, $\tau_0$, and Doppler shift, $\nu_0$. If $4N^2\tau_0\nu_0 \ll 1$ then by [4] and Theorem 1 the transfer matrix $\mathbf{H}(t,f)$ can be approximated by

$$\mathbf{H}(t,f) \approx \mathbf{D}(t,f) + \mathbf{R}(t,f)\left(\sum_{k=1}^{N}\mathbf{B}(t,f)^{k-1}\right)\mathbf{T}(t,f).$$

This approximation involves two types of errors. The first stems from the multiplications of multiple cascade operators which was investigated in Theorem 1 and the second is caused by truncating the infinite sum in (6). Truncation gives the error term

$$\mathbf{H}_{N+1:\infty}(t,f) = \mathbf{R}(t,f)\left(\sum_{k=N+1}^{\infty}\mathbf{B}(t,f)^{k-1}\right)\mathbf{T}(t,f). \quad (21)$$

Now since in a physical system $||\mathbf{B}(t,f)||^2 < 1$, the truncation error $\xi_N^2 := ||\mathbf{H}_{N+1:\infty}||^2$ is bounded as

$$\xi_N^2 \le ||\mathbf{R}(t,f)||^2 \left|\left|\left(\sum_{k=N+1}^{\infty}\mathbf{B}(t,f)^{k-1}\right)\right|\right|^2 ||\mathbf{T}(t,f)||^2$$
$$\le ||\mathbf{R}(t,f)||^2 \left(\sum_{k=N+1}^{\infty}||\mathbf{B}(t,f)^{k-1}||\right)^2 ||\mathbf{T}(t,f)||^2$$
$$= ||\mathbf{R}(t,f)||^2 \left(\frac{||\mathbf{B}(t,f)||^{N+1}}{1 - ||\mathbf{B}(t,f)||}\right)^2 ||\mathbf{T}(t,f)||^2 \quad (22)$$

which decays exponentially when $N \to \infty$. Thus given a measurement accuracy, $\epsilon$, there exists some $N_C$ such that $\xi_{N_C}^2 < \epsilon$. If $N_U \ge N_C$ the cascade approximation error caused by multiplication of transfer functions for cascades of length

greater than $N_C$ is negligible, and we can approximate $\mathbf{H}(t,f)$ with the limit result in [4],

$$\mathbf{H}_{0:\infty}(t,f) = \mathbf{D}(t,f) + \mathbf{R}(t,f)\left[\mathbf{I} - \mathbf{B}(t,f)\right]^{-1}\mathbf{T}(t,f).$$

This relation provides a significant numerical advantage when performing simulations of the wireless channel.

## IV. SIMULATION

We consider a V2V communication system transmitting in a tunnel with one transmitter, $T_1$, one receiver, $R_1$, and $N_S$ scatterers. We associate each vertex, $v$, in the time-varying propagation graph with a position vector $\mathbf{r}_v(t) \in \mathbb{R}^3$. The edge presence function can be deterministic or stochastic depending on the model specifications. For simplicity, we use a deterministic approach where an edge is present between to vertices if they are closer to each other than a predefined distance limit $d_{\text{lim}}$, i.e.

$$\rho((v,v'),t) = \begin{cases} 1 & \text{if } ||\mathbf{r}_v(t) - \mathbf{r}_{v'}(t)||_2 < d_{\text{lim}} \\ 0 & \text{otherwise.} \end{cases} \quad (23)$$

We use two distance limits, $d_B$ and $d_{DTR}$ for $(v,v') \in E_S$ and $(v,v') \in E_D \cup E_T \cup E_R$ respectively. Furthermore the edge presence function is chosen such that no scatterers on the same surface of the tunnel have edges connecting them. For the time-varying propagation graph the transfer function of each edge $e = (v,v')$ is then defined as

$$H_e(t,f) = \begin{cases} g_e(t,f)e^{i(\phi_e - 2\pi\tau(e,t)f)} & \text{if } e \in E \\ 0 & \text{otherwise,} \end{cases} \quad (24)$$

where $g_e(t,f)$ is a time-varying and frequency dependent gain, $\phi_e$ is a phase offset chosen uniformly in $[0; 2\pi)$ and $\tau(e,t) = \tau((v,v'),t) = ||\mathbf{r}_v(t) - \mathbf{r}_{v'}(t)||_2/c$ is the edge delay function, with $c$ the speed of light. We denote the delay from $v$ to $v''$ via $v'$ as $\tau_{(v-v'-v'')}(t) = \tau((v,v'),t) + \tau((v',v''),t)$, regardless of whether the journey exists or not. Furthermore we define a gain factor, $g(t) = 10^{\frac{\kappa\mu(E,t)}{20}}$, where $\mu(E,t) = \frac{1}{|E|}\sum_{e \in E}\tau(e,t)$. The gain of each edge is then defined as

$$g_{(v,v')}(t,f) = \begin{cases} \frac{1}{4\pi f\tau((v,v'),t)} & (v,v') \in V_T \times V_R \\ \left(\frac{1}{4\pi f\tau_{V_T-V_S-V_R}(t)}\right)^{1/2} & (v,v') \in V_T \times V_S \\ \left(\frac{1}{4\pi f\tau_{V_T-V_S-V_R}(t)}\right)^{1/2} & (v,v') \in V_S \times V_R \\ g(t)\sqrt{S_{(v,v')}(t)} & (v,v') \in V_S \times V_S \end{cases}$$

where $S_e(t) = \frac{1}{\sqrt{\text{odi}(e,t)}}$, and $\text{odi}(e,t)$ is the number of outgoing edges of the initial vertex of $e$ at time $t$.

We perform two simulations of $5\,\text{s}$ of driving with different movement patterns of the transmitter and receiver. In both setups the vehicles move linearly through the tunnel and we let the initial position of the transmitter and receiver be deterministic, such that the transmitter starts in front of the receiver. Furthermore the initial positions ensure there is $30\,\text{m}$ of tunnel behind the receiver in the beginning and $30\,\text{m}$ of tunnel in front of the leading vehicle at the end of the simulated time window. Thus allowing for the placement of scatterers on either side of the vehicles. The $N_S$ scatterers are split evenly

among the floor, ceiling and two walls of the tunnel and their position drawn uniformly within the region of interest. In all simulations the distance limit for inter-scatterer propagations is set to $36\,\text{m}$. Full model- and simulation parameters are listed in Table I.

Two setups (A and B) are compared. In Setup A the transmitter starts $120\,\text{m}$ in front of the receiver and both vehicles move at the same velocity of $108\,\text{km/h}$. In order to also include propagation journeys with four or less bounces including the direct propagation the distance limit, $d_{DTR}$, is set to $121\,\text{m}$. The resulting Power Delay Profile (PDP) and Doppler power Spectral Density (DSD) are seen in Figure 2(a) and 2(b). In Setup B the transmitter starts $50\,\text{m}$ in front of the receiver. The transmitter has a velocity of $60\,\text{km/h}$. The receiver has a velocity of $132\,\text{km/h}$, such that it overtakes the receiver and at the end of the simulated time window is $50\,\text{m}$ in front of the transmitter. The distance limit $d_{DTR}$ is set to $51\,\text{m}$. The PDP and DSD are seen in Figure 2(c) and 2(d).

The PDPs obtained for both setups exhibit a direct component followed by an exponentially decaying tail. In setup A, the delay of the direct component is constant since the transmitter does not move relatively to the receiver. In setup B, the direct component varies due to the relative movement of the transmitter and receiver. In both scenarios, the slope and magnitude of the tail are nearly the same regardless of the position of the vehicles and scatterers. Furthermore the appearances and disappearances of signal components due to the movement of the vehicles in relation to the fixed scatterers can be seen.

The DSDs clearly differ for the two setups. In setup A, the DSD includes a direct component situated at $0\,\text{Hz}$. In setup B, the direct component shows a clear change from positive to negative Doppler shift as the receiver overtakes the transmitter. For the presented setups, it is possible to track the development in Doppler frequency of individual propagation paths. The Doppler shifts of indirect components can be observed to transition from high to low values as the scatterers are passed by both transmitter and receiver.

It can be observed from the DSD in setup B, that the number of significant multipath components is largest when the transmitter is close to the receiver. Furthermore, DSDs of partial responses (not reported here), reveal that the behavior of Doppler shifts varies with interaction order. This is expected since the Doppler trajectory of a path is given by the positions of the first and last interaction point in a path. Accordingly, the temporally averaged DSDs of the full responses (not included here) have three peaks for setup A and four peaks for setup B. Finally, we remark that by increasing the number of scatterers further smears out both PDPs and DSDs.

## V. CONCLUSION

The proposed extension of the propagation graph framework to time-varying systems is built on the combination of the theory of dynamic graphs and the theory of linear time-variant operators. For this model construction, the time-variant transfer function is not available in closed-form. However, relying on an assumption of underspread operators, the closed-form
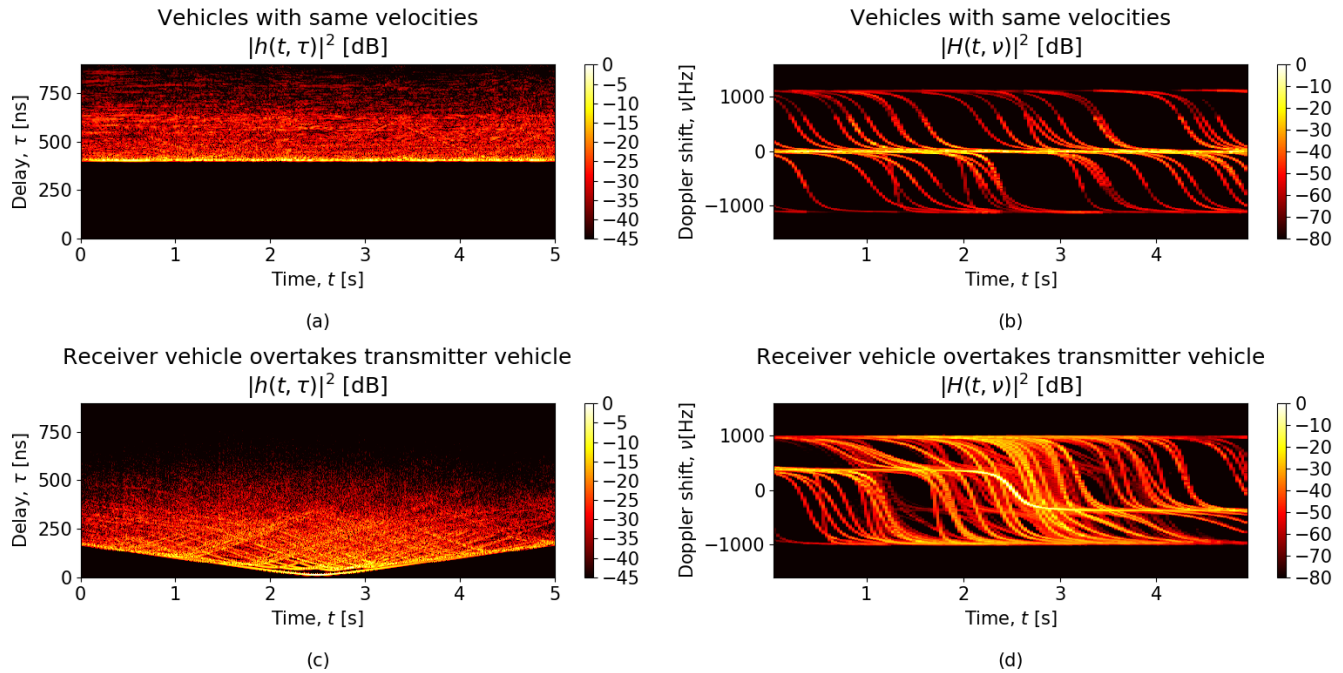
Fig. 2. Normalized time-varying PDP and DSD from simulations of V2V transmission in a tunnel environment. (a) PDP and (b) DSD for setup A when vehicles move with the same velocity. (c) PDP and (d) DSD for setup B when receiver vehicle overtakes transmitter vehicle.

TABLE I
SIMULATION PARAMETERS FOR A TUNNEL ENVIRONMENT WITH A MOVING
TRANSMITTER AND RECEIVER.

| Model parameters | Symbol | Setup A | Setup B |
|---|---|---|---|
| Environment | $\mathcal{R}$ | $[0, 255] \times [0, 11] \times [0, 7]\mathrm{m}^3$ | - |
| Number of scatterers | $N_S$ | 60 | - |
| $\mathbf{B}(t, f)$ distance limit | $d_B$ | $36.0\,\mathrm{m}$ | - |
| $\mathbf{D}(t, f), \mathbf{T}(t, f), \mathbf{R}(t, f)$ distance limit | $d_{DTR}$ | $121.0\,\mathrm{m}$ | $51.0\,\mathrm{m}$ |
| Tail slope factor | $\kappa$ | $-150$ | - |
| Initial transmitter position | $\mathbf{r}_T$ | $[156, 5.5, 1.5]\,\mathrm{m}$ | $[86, 3.6, 1.5]\,\mathrm{m}$ |
| Initial receiver position | $\mathbf{r}_R$ | $[36, 5.5, 1.5]\,\mathrm{m}$ | $[36, 7.2, 1.5]\,\mathrm{m}$ |
| Velocity of transmitter | $\mathbf{v}_T$ | $[30, 0.0, 0.0]\,\mathrm{m/s}$ | $[16.6, 0.0, 0.0]\,\mathrm{m/s}$ |
| Velocity of receiver | $\mathbf{v}_R$ | $[30, 0.0, 0.0]\,\mathrm{m/s}$ | $[36.6, 0.0, 0.0]\,\mathrm{m/s}$ |
| Speed of light | $c$ | $3.0 \cdot 10^8\,\mathrm{m/s}$ | |
| Input signal | $X$ | Unit power Hann pulse | |
| Frequency range | $F$ | $[5.36, 5.84]\,\mathrm{GHz}$ | |
| Frequency samples | $M_F$ | 769 | |
| Time range | $\mathcal{T}$ | $[0, 5]\,\mathrm{s}$ | |
| Time samples | $M_{\mathcal{T}}$ | 16000 | |

expression available for the time-invariant graphs provides an approximation for the instantaneous transfer function. The error of this approximation is bounded and thus the approximation is valid under conditions on the effective support of the delay-Doppler spread function of the recursive operator. The approximation can be used to simulate the response of the time-varying propagation graph. In the numerical examples given here, we consider a vehicle-to-vehicle tunnel scenario. We find that the model includes both early signal components as well as a later reverberation tail.

## ACKNOWLEDGMENT

## REFERENCES

[1] J. Karedal, F. Tufvesson, N. Czink, A. Paier, C. Dumard, T. Zemen, C. F. Mecklenbräuker, and A. F. Molisch, "A geometry-based stochastic mimo model for vehicle-to-vehicle communications," *IEEE Trans. on Wireless Communications*, vol. 8, no. 7, pp. 3646–3657, July 2009.

[2] T. Pedersen and B. H. Fleury, "A realistic radio channel model based on stochastic propagation graphs," in *Proceedings 5th MATHMOD Vienna – 5th Vienna Symposium on Mathematical Modelling*, vol. 1,2, Feb. 2006, p. 324, ISBN 3–901608–30–3.

[3] T. Pedersen and B. Fleury, "Radio channel modelling using stochastic propagation graphs," in *Proc. IEEE International Conf. on Communications ICC '07*, Jun. 2007, pp. 2733–2738.

[4] T. Pedersen, G. Steinböck, and B. H. Fleury, "Modeling of reverberant radio channels using propagation graphs," *IEEE Trans. Antennas and Propagation*, vol. 60, no. 12, pp. 5978–5988, Dec. 2012.

[5] T. Zhou, C. Tao, S. Salous, Z. Tan, L. Liu, and L. Tian, "Graph-based stochastic model for high-speed railway cutting scenarios," *IET Microwaves, Antennas Propagation*, vol. 9, no. 15, pp. 1691–1697, 2015.

[6] W. Cheng, C. Tao, L. Liu, R. Sun, and T. Zhou, "Geometrical channel characterization for high speed railway environments using propagation graphs methods," in *16th International Conference on Advanced Communication Technology*, Feb 2014, pp. 239–243.

[7] M. Gan, G. Steinböck, Z. Xu, T. Pedersen, and T. Zemen, "Non-stationary vehicle-to-vehicle channel model for tunnels with reduced numerical complexity," 2017, submitted to IEEE Trans. Vehicular Techn.

[8] A. Casteigts, P. Flocchini, E. Godard, N. Santoro, and M. Yamashita, "On the expressivity of time-varying graphs," *Theoretical Computer Science*, vol. 590, pp. 27–37, 2015.

[9] W. Kozek, "Matched weyl-heisenberg expansions of nonstationary environments," Ph.D. dissertation, Vienna University of Technology, September 1996.

[10] L. A. Zadeh, "Frequency analysis of variable networks," *Proc. I.R.E.*, vol. 38, pp. 291–299, 1950.

[11] P. Bello, "Characterization of randomly time-variant linear channels," *IEEE Trans. Commun. Systems*, vol. 11, no. 4, pp. 360–393, dec 1963.